

# The nitrogen-vacancy center in diamond revisited

N. B. Manson, J. P. Harrison and M. J. Sellars

Laser Physics Center, Research School of Physical Sciences and Engineering  
Australian National University, Canberra, A.C.T., 0200, Australia

(Dated: April 6, 2019)

Symmetry considerations are used in presenting a model of the electronic structure and the associated dynamics of the nitrogen-vacancy center in diamond. The model accounts for the occurrence of optically induced spin polarization, for the change of emission levels with spin polarization and for new measurements of transient emission. The rate constants given are in variance to those reported previously.

PACS numbers: 42.50.Gy, 42.50.Nn, 76.30Mi

## I. INTRODUCTION

Since the nitrogen-vacancy (N-V) center in diamond has been detected at a single site level [1, 2, 3] the center has attracted attention for various quantum information processing applications. For example, the center has been used as a single photon source for quantum cryptography [4, 5] and work in this area has included impressive demonstrations [6]. Another area of interest results from the center having a non-zero spin ground state. The ground state spin can be the qubit and the optical transitions utilized for readout and for qubit manipulation. There are again impressive demonstrations in this area [7, 8, 9, 10, 11]. With these successes and additional programs under development it might be expected that the properties of the N-V center are well understood. However, this is not the case. Despite the extensive publications the center is not well understood and the literature contains many inaccuracies. The purpose of this paper is to re-visit our knowledge of the nitrogen-vacancy center, provide an account of the electronic energy levels and more particularly explain the dynamics of the center under optical excitation.

## II. NITROGEN-VACANCY CENTER

The N-V center occurs in diamond containing single substitutional nitrogen when irradiated and annealed [12, 13]. Electron irradiation with energies greater than 200 keV creates vacancies [14]. The vacancies are mobile at 800 C and can become trapped adjacent to the nitrogen impurities. The nitrogen-vacancy complex formed has a strong optical transition with a zero-phonon line at 1.945 eV (637 nm) accompanied by a vibronic band at higher energy in absorption and lower energy in emission. The zero-phonon line has been studied by Davies and Hamer [13]. They have studied the effect of uniaxial stress and from the splitting and polarization they established that the transition is associated with an orbital A-E transition at a site of trigonal symmetry. The trigonal symmetry is consistent with an adjacent nitrogen-vacancy pair with  $C_{3v}$  symmetry. In other studies using optical excitation Loubser and van Wyk detected ESR

signals of a spin polarized triplet ( $S = 1$ ) [15]. The ESR they observed was associated with a center having trigonal symmetry and the magnitude of the optically induced signal was found to vary with wavelength in correspondence with the strength of the A-E optical transition. Hence, the center was attributed to the same nitrogen-vacancy complex. With an integer spin ( $S = 1$ ) the center must have an even number of electrons and it is taken that the neutral nitrogen-vacancy complex with five electrons has acquired an additional electron from elsewhere in the lattice, probably from another substitutional nitrogen atom. There will then be six electrons occupying the dangling bonds of the vacancy complex [15]. Loubser and van Wyk proposed that the spin polarization arises from a singlet electronic system with inter-system crossing to a spin level of a meta-stable triplet. However, it was established from hole burning [16], optically detected magnetic resonance [17], ESR [18] and Raman heterodyne measurements [19] that the triplet is the ground state rather than a meta-stable state. Therefore, their model has to be modified to give a  $^3A$  ground state and a  $^3A$   $^3E$  optical transition. The optically induced spin polarization can still arise from inter-system crossing and an account is given in this paper.

The six electrons occupy the dangling bonds associated with the vacancy complex. A discussion of this situation is included in a treatment by Lenef et al. [20]. Although they did not adopt the six electron model [21] they did give a very useful general treatment including the six electron situation and their presentation allows the present discussion to be brief and more descriptive. The dangling bonds are formed from  $sp^3$  orbitals of the carbon and nitrogen atoms and in a vacancy approximating  $T_d$  symmetry these can be combined to form  $a_1$  and  $t_2$  molecular orbitals with  $A_1$  and  $T_2$  symmetry, respectively [22]. From symmetry and charge overlap considerations the  $a_1$  is considered to be lower in energy and the  $t_2$  higher. With six electrons  $a_1^2 t_2^4$  will be the lowest energy configuration and this can also be described as a  $\frac{1}{2}$  hole system. When the  $T_d$  symmetry is lowered to trigonal the  $t_2$  orbital will be split to give, in  $C_{3v}$  notation, an  $a_1$  and  $e$  orbital. The  $e$  hole is lower in energy and, hence, the lowest energy configuration will be  $e$ , next lowest  $a_1$  and the  $a_1^2$  highest. The spin-orbit wave func-

tions for the  $e^2$  configuration give  $^3A_2$ ,  $^1A_1$  and  $^1E$  states and the  $ea_1$  configuration  $^3E$  and  $^1E$  states. The  $a_1^2$  gives an  $^1A_1$ . The optical transition is associated with triplets and so the ground state is attributed to the  $^3A_2$  ( $e^2$ ) state and the excited state to the  $^3E$  ( $ea_1$ ) state. There are singlets  $^1A_1$  ( $e^2$ ) and  $^1E$  ( $e^2$ ) and  $^1E$  ( $a_1e$ ) which could lie in the same energy range as the triplets. The  $^1A_1$  ( $a_1^2$ ) lies higher. It has been assumed that the  $^1A_1$  ( $e^2$ ) lies between the triplets and the present treatment accepts this assertion and will be shown to be consistent with observation. The possibility of intermediate  $^1E$  level(s) will be discussed.

The energy of the  $^3A_2$ ,  $^3E$ ,  $^1A_1$  states are determined by the above bonding consideration. We consider how these states are effected by spin-orbit and spin-spin interaction. The ground state is an orbital singlet and is only affected by spin-spin interaction. In trigonal symmetry it is split into a singlet,  $A_2, S_z >$  with symmetry  $A_1$ , and doublet,  $A_2, S_x >$ ,  $A_2, S_y >$  with symmetry  $E$ . The  $^3E$  excited state is an orbital doublet and the dominant splitting is by axial  $L_z S_z$  spin-orbit interaction and gives three two-fold degenerate states;  $E$ ,  $E'$ , and an  $(A_1, A_2)$  pair. The non-axial spin-orbit interaction is small and will be neglected at present. The spin-spin interaction is perhaps also smaller than the axial spin-orbit interaction but regardless does not cause any mixing of the wave functions. These states and the symmetry adapted wave functions are then as given in Fig 1(a). We are principally concerned with the wave-functions and will not consider the splitting in detail. In this approximation it should be noted that states with  $S_z$  spin projection are not mixed with the spin states with  $S_x$  and  $S_y$  spin projection. The  $A_2 \rightarrow E$  transition is orbitally allowed and as spin projection is not changed by the electric dipole operator the optical transitions will be the same strength for each of the spin projections (shown as solid vertical arrows in Fig 1(a)). There are no transitions involving a change of spin and it can be concluded that optical cycling of the  $^3A_2 - ^3E$  transition will not result in change of spin projection or result in any spin polarization. This situation does not change when considering vibronic interactions as spin projection is conserved.

Spin-orbit interaction mixes singlets and triplets which transform according to the same irreducible representation. The mixing provides an avenue whereby symmetric vibration can cause a population relaxation between the mixed singlets and triplets. The symmetry considerations, therefore, determine the allowed inter-system crossing and these are also shown in Fig 1(a). Where there is only a  $^1A_1$  singlet level the inter-system crossing is restricted to states that transform as  $A_1$  irreducible representations. There can be excitation of population out of the  $E$  ground state level with  $S_x$  and  $S_y$  spin projections to the  $A_1$  spin-orbit level of the  $^3E$  state. Population in this state can decay via the singlet to the  $S_z$  spin projection of the ground state. Such an excitation and decay, therefore, causes a re-orientation of the ground state spin projection and with continuous excitation pop-

ulation can be transferred to the ground  $S_z$  spin state. This is consistent with the preferred spin orientation [23]. With these selection rules, assuming the optical induced spin polarization is faster than spin-lattice relaxation, the spin polarization would be 100% but this is not what is observed.

The extra consideration is the non-axial  $(L_x S_x + L_y S_y)$  spin-orbit interaction which we have previously neglected. This spin-orbit term causes a mixing of the two  $^3E$  states (denoted  $E$  and  $E'$ ) transforming as an  $E$  irreducible representation. These states have different  $S_z$  and  $S_x, S_y$  spin projections and, hence, the mixing gives rise to optical transitions that do not conserve spin (dashed arrows in Fig 1). The transitions are observed in hole burning spectra [16, 24, 25, 26] and are the transitions that limit the degree of spin polarization that is achieved. It is anticipated that the strength of the non-axial spin-orbit interaction is small. The non-axial spin-orbit term would be zero in  $T_d$  and is only allowed through the lowering of the symmetry to  $C_{3v}$ . The interaction is, therefore, anticipated to be small and the non-spin conserving optical transitions weak. Although weak the transitions play an important role in limiting the saturation spin populations.

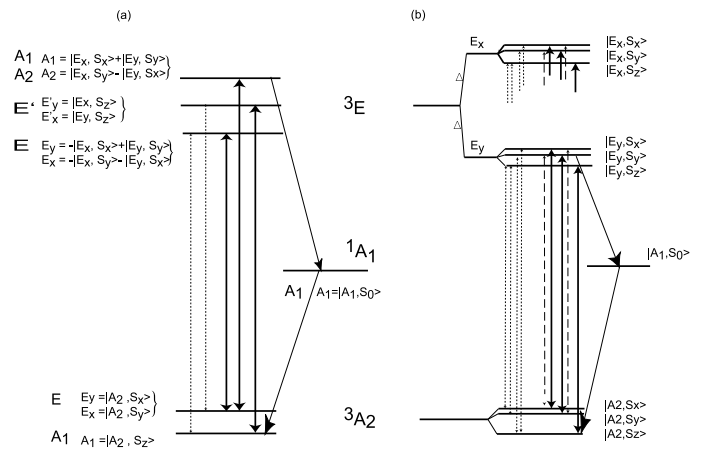


FIG. 1: (a) Energy levels of the N-V center in  $C_{3v}$  symmetry. The excited state is split by spin-orbit interaction whereas the ground state is split by spin-spin interaction (not shown to scale). The figure gives the symmetry adapted wavefunctions. The solid arrows indicate the spin-allowed optical transitions. The dashed arrows indicate weak transitions which are allowed through the mixing of the  $(^3E)E$  and  $(^3E)E'$  basis states by transverse spin-orbit interaction. The diagonal arrows give inter-system crossing allowed by spin-orbit interaction. (b) Energy levels and wave functions of the N-V center in the presence of a strain field. The wave functions are appropriate for a strain field perpendicular to a refection plane. The transitions are derived from those allowed in (a).

We briefly consider the situation where a  $^1E$  state(s) lies between the  $^3A_2$  and  $^3E$ . If this were the case there could be symmetry allowed relaxation from the excited triplet  $(^3E)E$  and  $(^3E)E'$  states to such an intermediate

ate  $^1E$  singlet state. However, using the two hole description the relaxation is found to be forbidden in the case of the triplet  $(^3E)E'$  state (cancellation of terms for a  $^1E$  ( $a_1e$ ) and forbidden for one electron operators for  $^1E$  ( $e^2$ ) states) implying that there will still not be population transfer out of states with  $S_z$  spin projection. There can be relaxation from the other triplet  $(^3E)E$  state involving the  $S_x, S_y$  spin projections to a  $^1E$  level. Given that there is also an intermediate  $^1A_1$  there can be two alternate situations depending on the ordering of the  $^1A_1$  and  $^1E$  singlet levels. Should the  $^1E$  state lie below the  $^1A_1$  level the decay from the lowest singlet, the  $^1E$ , will be to the  $(^3A_2)E$  component of the ground state. This state has a  $S_x, S_y$  spin projection and the optical cycling will have had no consequence implying no change in spin orientation. However, if the  $^1E$  state lies above the  $^1A_1$  level there will be radiative (or non-radiative) decay to the lower singlet level, the  $^1A_1$ , followed by the relaxation, as discussed in the previous paragraph, to the  $S_z$  spin projection of the ground state. This process will lead to the same spin change and spin polarization as before and the simple consequence of involving the  $^1E$  singlet is that the total ( $^1A_1$  plus  $^1E$ ) spin polarization process will be more efficient. Thus, if there is an intermediate  $^1E$  state, to be consistent with observation it must lie at an energy higher than the  $^1A_1$  state. It is recognized that this order is in disagreement with calculated energy levels [28]. However, there is an appeal of including a higher single  $^1E$  state as it could lie close to the excited triplet level and the  $^1A_1$  close to the ground state thus accounting for the relatively fast inter-system crossing reported below. However, there is no fundamental difference in the dynamics and it is sufficient in this work to restrict the discussion to one singlet level, a  $^1A_1$ .

It is common for there to be strain in diamond and it is worth considering the consequence to the energy levels and the associated dynamics. There will be no fundamental change with axial strain as all it gives is a uniform shift of the energy levels and no change of the wave functions or the dynamics. However, the component of the strain at right angles to the axis of the center lowers the symmetry and the extra crystal field lifts the orbital degeneracy of the excited state to give two orbital non-degenerate states denoted  $E_x$  and  $E_y$  [20]. We consider the case where this strain splitting is larger than the spin-orbit interaction. Where the strain retains a reflection plane the  $Z, X, Y$  axes will be determined by symmetry. The wave functions for this situation are as given in Fig 1(b). In the limit of small non-axial spin-orbit interaction there is still little mixing of the  $S_x, S_y$  spin states with the  $S_z$  spin states. The transitions and inter-system crossing can be determined from the parent state and are shown in Fig 1(b). The spin allowed transitions will have near the same strength as in the zero strain case but they are now totally polarized. The only minor change is loss to the dashed transitions between the states with different  $S_x$  and  $S_y$  projections. These arise where the strain is not sufficient to totally quench the effect of the diagonal

spin-orbit interaction. A more significant effect is in the strength of the non-spin-conserving transitions induced by non-axial spin-orbit interaction. They will become significantly stronger as the separation of the  $S_z$  and  $(S_x, S_y)$  states mixed is much smaller. When the strain does not retain reflection symmetry the effective X and Y axis may be different between ground and excited states and all transitions and inter-system crossings will become allowed in principle (no symmetry restrictions). However, the selection rules will be dominated by those allowed in zero order and the perturbation approach in Fig 1(b) is anticipated to give a reasonable approximation to the dominant excitation and decay channels.

Which of the diagrams Fig 1(a) or Fig 1(b) (or an intermediate case) is appropriate depends on the relative magnitude of the stress and the spin-orbit interaction. Spin-orbit for the carbon atom is known to be a few  $\text{cm}^{-1}$  (200 GHz) and a spin-orbit splitting of 1  $\text{cm}^{-1}$  (30 GHz) was obtained for the  $^3E$  state from optical magnetic circular dichroism measurements [16]. With a concentration of N-V centers it is common for the inhomogeneous width of the zero-phonon line to have a width of several hundred GHz and significant part of this width can be attributed to stress. The stress splitting is, hence, larger than the strength of the spin-orbit interaction and Fig 1(b) will be the appropriate energy scheme. There will be fast vibrational decay from the upper branch to the lower branch ( $E_x$  to  $E_y$  in Fig 1(b)) and the associated structure will not be resolved as the levels will be lifetime broadened. The structure in the lower levels are frequently obtained in hole burning measurements when the laser frequency is on the low energy side of the zero-phonon line [16, 24, 25, 26] but the structure [27, 29] has not been satisfactorily explained. Little structure is obtained for absorption at the center of the zero-phonon line and, hence, there is no experimental knowledge of the energy levels associated with centers corresponding to Fig. 1(a). Therefore, the current situation is that the strength of the interactions in the excited  $^3E$  state are not well established and this remains an outstanding issue for a full understanding of the N-V center.

The dynamics associated with optical excitation can be determined without detailed knowledge of the excited state energy levels. This is because from the above discussion it can be seen that the system can be reasonably quantized by its spin projection  $S_z$  or  $(S_x, S_y)$  and this is not altered by stress. The dynamics are largely determined by the crossing between these two spin projections and the symmetry considerations give the two main mechanisms. These are through the inter-system crossing via the singlet and through the weak non-spin-conserving optical transitions. The effective energy scheme is given in Fig 2 where the  $S_z$  states are shown on the left and the  $(S_x, S_y)$  on the right. The singlets are drawn centrally. Spin polarization involves displacement of population from the states on the right to the states on the left. The transitions including those that change the spin projection are shown as solid lines as determined by the

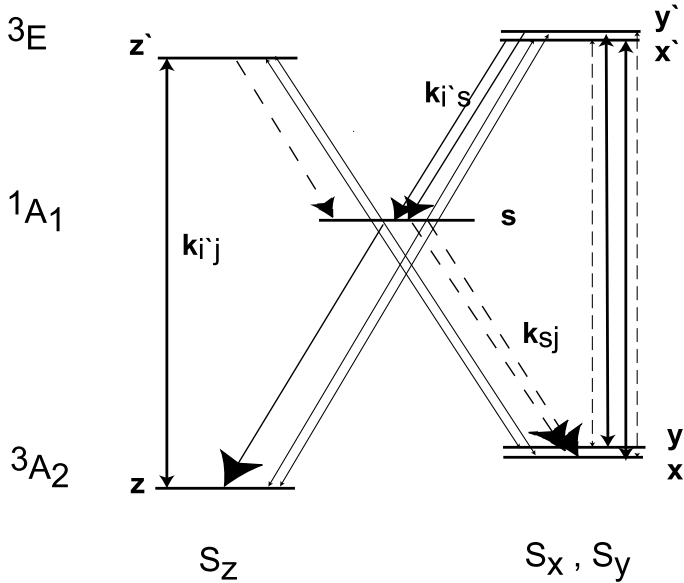


FIG. 2: Energy levels for a perturbed N-V center. The significant energy levels of Fig.1(b) are re-drawn to highlight the inter-system crossing. All the radiative and non-radiative transitions are shown. The allowed transitions considered in the text are shown by solid arrows. The dashed vertical arrows on the right are allowed but can be taken to be zero for present experiments. Also the inter-system crossing indicated by the dashed arrows are zero in first order.

parent states in  $C_{3v}$  symmetry. For completeness other transitions allowed in low symmetry are shown as dashed lines. The low symmetry situation is similar to that proposed by others [10, 30, 31] and to assist comparison we adopt their shortened notation. The ground spin states are denoted as  $x$ ,  $y$  and  $z$ ; the excited triplet states as  $x'$ ,  $y'$  and  $z'$  and the singlet level as  $s$ . In the following experiments we determine the values of the parameters using bulk samples.

### III. EXPERIMENTAL DETAILS

Several type 1b diamonds were used in these studies. They were irradiated with energetic electrons ( $> 1 \text{ MeV}$ ) and annealed. The nitrogen-vacancy concentrations varied from  $3 \times 10^{18}$  per  $\text{cm}^3$  to  $10^{17}$  per  $\text{cm}^3$  and there was no indication that the dynamics of the optical cycle varied significantly for concentrations in this range.

The experiments involve transient and CW excitation studies using a frequency doubled Nd:YAG laser. The excitation wavelength is 532 nm which is near the peak of the  $^3\text{A}_2 \rightarrow ^3\text{E}$  absorption band. The emission was detected by a S-20 photomultiplier or pin diode with a response time of 30 ns. With the exception of the measurement of the spectrum the emission wavelength detected was selected using absorptive filters.

The studies involved three different excitation and detection geometries. For low level excitation the intensity

was determined from the laser power and the beam diameter. The emission at  $45^\circ$  was focussed on the pin diode. For high intensity measurements a confocal arrangement with an oil immersion objective was used. The excited diameter was 0.2 micron with the emission spot focussed onto a pinhole. A 1 mW beam gave an estimated power density of  $2 \times 10^6 \text{ W/cm}^2$ . With the small excitation and detection volumes the signals were weak and long collection times were required to obtain satisfactory signal to noise ratios. The majority of the measurements were taken with a third geometry where satisfactory signals could be obtained more rapidly. The light was focused with a microscope objective and the back emission collected by the same objective. For the same laser power the intensity at the sample was approximately two orders of magnitude lower than that obtained with oil immersion objective and it required a 100 mW laser beam to obtain a maximum intensity of  $2 \times 10^6 \text{ W/cm}^2$ . The unsatisfactory feature of this geometry is that the intensity was not constant over the collected volume.

At low intensities where slow ( $> 1 \text{ ms}$ ) responses were obtained the light was gated with a mechanical chopper whereas for the fast speeds associated with the high intensities the light was gated using two acousto-optic modulators in series. The rise time of the A-O modulators is 30 ns. When gating on there was a weak component that lasted for a few nanoseconds. However, no measurements were taken when gating the light off.

### A. Preliminary measurements

The emission of the N-V center has been reported on many occasions. The general characteristics are shown in Fig.3. Near room temperature the emission gives a band stretching from 630 nm to 800 nm with vibrational structure and a weak zero-phonon line at 637 nm (Fig.3(a)). Cooling has little effect on the vibronic absorption band [32] and consequently there is little change in the amount of light absorbed from the laser beam when using an excitation wavelength within the vibronic band. Consistent with this, the total emission does not show a significant change when the temperature is lowered (inset in Fig.3(a)). The most obvious change in cooling to low temperatures is that the zero-phonon line becomes sharper and more prominent (Fig.3(b)). The Huang-Rhys factor is 3.7 with only 2.7 percent of the transition strength being associated with the zero-phonon transition [32]. At high excitation densities there can be photoionization of the N-V center of interest and the creation of the neutrally charged  $\text{N-V}^0$  center [33, 34]. This center has a zero-phonon line at 575 nm with a vibronic band to lower energy [35]. The increased contribution of this center at high intensities is illustrated in Fig.3(b).

As discussed earlier the N-V center exhibits optically induced spin polarization of the ground state triplet and there is a change of the emission intensity associated with this polarization. The change is illustrated in Fig.4. In

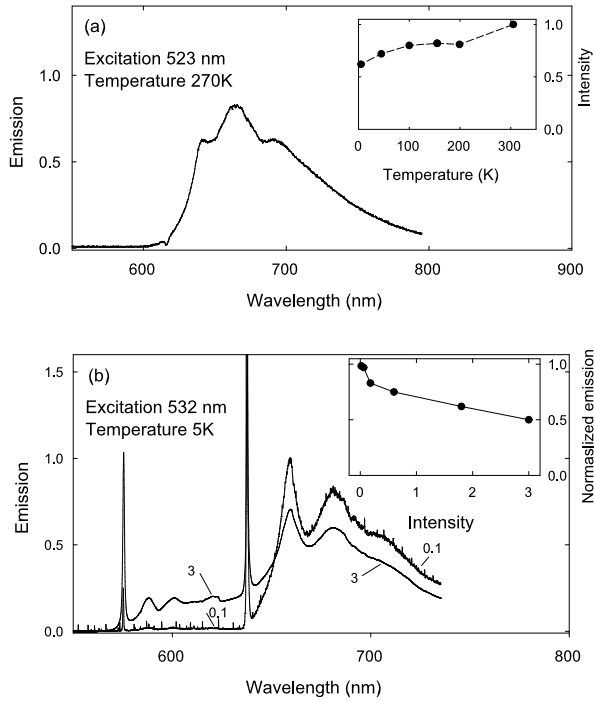


FIG. 3: Spectral characteristics of the N-V Center. (a) Emission spectra of a diamond containing a high concentration of N-V centers measured near room temperature using low excitation densities of  $1 \text{ W/cm}^3$ . Insert: the variation of the N-V emission at 666 nm as a function of sample temperature. (b) Low temperature emission spectra of the N-V center measured with various excitation densities (from reference [33]). Insert: variation of N-V emission intensity as a function of excitation energy density (units of  $1 \times 10^5 \text{ W/cm}^3$ ). Emission normalized to excitation intensity.

the dark the sample becomes unpolarized and when exciting the emission has an initial intensity level A. After exciting for a period the sample becomes polarized and the strength of the emission increases to a second value B (Fig. 4(a)). The rate at which the emission increases from the level A to B is linearly dependent on the excitation intensity. Should the sample be in the dark for a period less than the spin-lattice relaxation time ( $T_1$ ) the initial emission level will be at a value between A and B and varying the dark period varies this level. This variation of emission level with the duration in the dark can be used to establish the spin-lattice relaxation time and measurements of this type are shown in Fig. 4(b). The A/B ratio is of considerable interest. To ensure a satisfactory measurement it is necessary to have the sample in the dark for a period long compared to  $T_1$  whereas to obtain the saturation value B the intensity has to be suf-

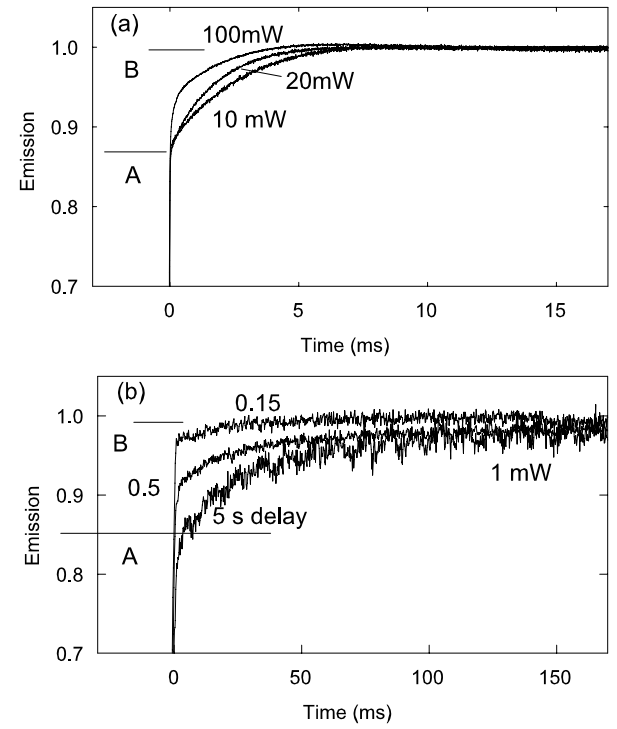


FIG. 4: Emission obtained when gating on excitation at time 0. The excitation is at 532 nm and is gated with a mechanical shutter. (a) Response for various laser powers; 10 mW corresponds to an intensity of  $1 \text{ W/cm}^2$ . The emission increases to an initial value A, 86% of its final value B. The rate of increase of the emission to its final CW value B depends on intensity of excitation. Sample has spin-lattice relaxation time of 100 ms and sample held in dark for 500 ms prior to excitation. (b) Responses for various periods in the dark. For these traces the sample is cooled and the spin-lattice relaxation time is increased to 500 ms.

cient to obtain the higher emission level within a time short compared to  $T_1$ . A decrease of the spin polarization through spin diffusion must also be avoided. When meeting these conditions the A/B ratio is 0.86 ± 0.02.

## B. Dualpulse measurements

The first series of measurements involves intense excitation with the delay between two pulses varied. These measurements utilized the confocal arrangement with oil immersion and intensities of  $10^6 \text{ W/cm}^2$ . The repetition rate was 10 kHz. The results are shown in Fig. 5(a). In the figure the response associated with the first pulse of every pair is overlapped whereas the emission associated with the second pulse is displaced as the delay between

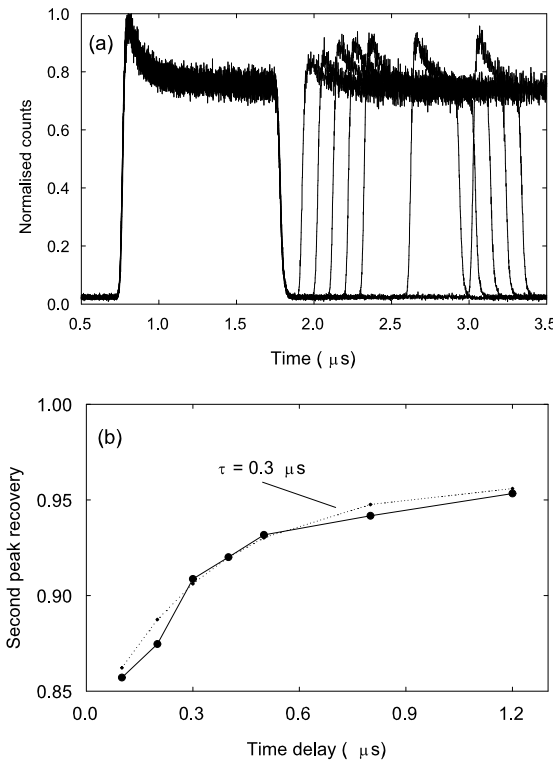


FIG. 5: Emission response to a double light pulse (a) The emission is shown with various delays between the two pulses. The responses for the first pulses all overlap whereas the second pulse is delayed by the dark period. The peak associated with the second pulse recovers with the dark period and the height of this pulse is plotted in (b) as a function of the duration in the dark. The dashed curve illustrates the response for a  $0.3 \mu\text{s}$  recovery rate. The repetition rate of the pulse pair was 10 kHz. The intensity of the excitation was  $3 \times 10^6 \text{ W/cm}^2$ .

the pulses is varied. Every pulse exhibits an initial peak followed by a decay within a  $\mu\text{s}$  to a lower level. For the first pulse the peak height is  $1/3$  that of the equilibrium signal. When the light is gated off a period in the dark is required before the second pulse gives a peak and the peak height increases as the dark period is increased. This recovery has two components and the faster recovery is shown to have a response time of  $0.3 \mu\text{s}$  (Fig. 5(b)). There is a slower recovery over the  $100 \mu\text{s}$  between pulses and we will comment on this slower recovery later.

For the second series of measurements the emission is obtained for a pulse pair of  $1 \mu\text{s}$  duration separated by  $1 \mu\text{s}$  but with long delays between the pulse pairs. The measurements were made using the alternate geometry where the excitation and detection involved a larger but

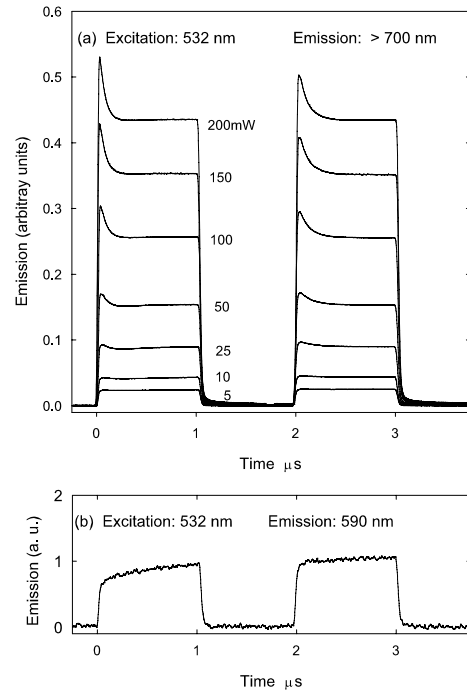


FIG. 6: Emission of the N-V center for a pair of square wave excitation pulse of light at 532 nm. The light is focused with a microscope objective and for 100 mW the intensity is  $2 \times 10^6 \text{ W/cm}^2$ . The back scattered emission is detected using a (a) 700 nm long pass filter, (b) 100 nm band pass filter at 590 nm.

less well defined volume. The period between pairs ( $> 10 \mu\text{s}$ ) was chosen to be much larger than ground state spin-lattice relaxation time,  $T_1$  ( $1 \mu\text{s}$ ). The intention is for the system to be unpolarized at the start of the first pulse but polarized at the start of the second pulse. Fig. 6(a) shows the results of the emission response for pulse pairs for laser powers from 5 mW to 200 mW corresponding to estimated intensities of  $10^5 \text{ W/cm}^2$  to  $4 \times 10^6 \text{ W/cm}^2$ . The emission is restricted to longer wavelengths ( $> 700 \text{ nm}$ ) to avoid including emission from  $\text{N-V}^0$  centers. The emission of the  $\text{N-V}^0$  center by itself was also obtained by detecting the emission at 590 nm using a narrow band filter. This emission is shown in Fig. 6(b).

The responses in Fig. 6(a) show peaks at the start of each pulse and the magnitude increases with intensity. The peak height of the second pulse is consistently several percent lower than that of the first. Also the decay rates are different for the two pulses, the first being faster than the second.

The effect of applying a weak magnetic field of a few hundred gauss was also recorded. The response to a pair

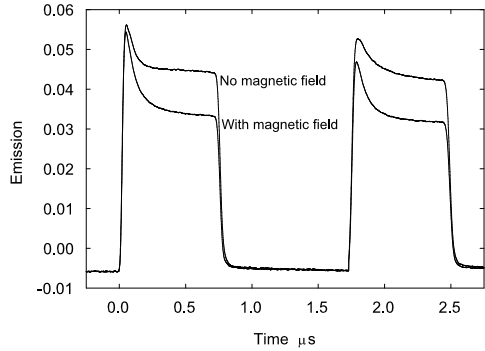


FIG . 7: Emission of the N-V center for a pair of square wave excitation pulses of light at 532 nm with laser intensity of 100 mW . No magnetic field is applied in the case of the upper trace and corresponds to the 100 mW trace in Fig 6. For the lower trace a field of 500 gauss is applied in a random direction (not aligned with an axis of any center).

of intense (100 mW) excitation pulses at 532 nm were measured both with and without the magnetic field applied in a random direction (Fig.7). In comparing the two traces there are three significant differences. The first emission peak is almost the same for the two traces but the subsequent decay is to a much lower level when the magnetic field is applied. With the second pulse there is a significant difference in the peak heights, being lower with the field is applied. Also with the second pulse the decay to the lower level is faster when the magnetic field is applied.

#### IV . RELAXATION AND INTER-SYSTEM DECAY RATES

The dynamics scale with the lifetime of the excited state and various values have been reported in the literature. Collins et al [36] have obtained values of 12.9

0.1 ns for a natural diamond and 11.6 0.1 ns for a synthetic diamond. Leneff et al. [20] has also obtained a

measure of 12.96 0.14 ns obtained in relation to photon echo measurements. A value of  $\tau = 13$  ns is adopted here. The radiative rate constants are, hence,  $k_{x^0x} = k_{y^0y} = k_{z^0z} = 77 \times 10^6 \text{ s}^{-1}$ . (The present experiments are not sensitive to the dashed vertical transitions in Fig 2 between the  $x, x'$  and the  $y, y'$  states and the associated rate constants can be taken to be zero, ie  $k_{x^0y^0} = k_{y^0x^0} = 0$ ). It is noted that the present model indicates that there should be two components to the emission decay associated with excited states, one with  $z'$  and one with  $x', y'$ . The emission from  $z'$  excited state has the slower decay rate and dominates when the system is spin polarized, perhaps explaining why the two values (differing by only 30%) have not been detected. Two components of 9 ns and 2 ns have been observed by Hanzana et al [37] but the measurements are inconsistent with previous values and require further investigations.

The increase in emission from a level A to a level B can be used to establish the fraction of the population transferring into the singlet. For example the 14% emission change between having all the population in the  $z$  spin ground state and having the population evenly distributed between the three spin states implies 27% of the population from each of the  $x', y'$  excited spin states transferring non-radiatively to the singlet,  $s$ . This has to be increased to 39% to allow for the incomplete spin polarization reported below. The inter-system crossing rates are then  $k_{x^0s} = k_{y^0s} = 30 \times 10^6 \text{ s}^{-1}$ . In correspondence with the model, the inter-system crossing from the  $z'$  state to the singlet is taken to be zero and, hence,  $k_{z^0s} = 0$ .

For the low intensities no population is maintained in the singlet. This is changed at high intensities and the transient emission displays different characteristics. With population being stored in the singlet level there is a drop in emission and this is observed in all of the two-pulse experiments (Figs.5, 6 and 7). There will be no initial peak if the excitation is gated on and off within a few ns as there will be no change in the singlet population. The recovery of the peak requires a period in the dark (Fig.5) and the time required corresponds to the rate at which population decays from the singlet to the ground state. The value of the singlet lifetime obtained from this peak recovery is 0.3 s and this gives  $k_{sz} = 3.3 \times 10^6 \text{ s}^{-1}$ . As in the model we take  $k_{sx} = k_{sy} = 0$ .

In a recent paper we have reported that the maximum spin polarization obtained for an ensemble under continuous excitation is 80% [38]. This means that the probability of optically transferring spin projection from the  $z$  spin state to an  $x, y$  spin is 1/4 of the above process giving rise to the spin polarization. The mechanism is attributed to the non-spin conserving optical transitions (diagonal arrows between triplet levels in Fig 2) and implies that the rate constants are  $k_{zx^0} = k_{zy^0} = k_{x^0z} = k_{y^0z} = 1.5 \times 10^6 \text{ s}^{-1}$ . Loss of spin polarization could also arise from the reverse inter-system crossing via the singlet level. However, the model predicts that the rate is zero,  $k_{z^0s} = 0$  and as given previously the decay from the

singlet to the x and y ground states are also zero.

## V. RATE EQUATIONS

In the previous section estimates of the parameters of the model in Fig 2 have been obtained from simple experimental observations. By adopting these parameters we can determine the populations and the emission for any optical field by solving the classical rate equations:

$$dn_i/dt = \sum_j (k_{ji}n_j - k_{ij}n_i)$$

where  $n_i$  is the population of level  $i$  ( $i = z, x, y, z', x', y'$ , s), and  $k_{ij}$  gives the rate for the  $i \rightarrow j$  transition. The significant parameters associated with the optical transitions are:

$$(k_{z^0z}, k_{x^0x}, k_{y^0y}), (k_{x^0z}, k_{y^0z}, k_{z^0x}, k_{z^0zy}), (k_{x^0y}, k_{y^0x})$$

where the values within brackets are equal in first order. The related optically driven terms are obtained by setting  $k_{ij} = k \cdot k_{ji}$  where  $k$  indicates the strength of the optical pumping.  $k = 1$  corresponds to the case where the optical pumping rate of the allowed transitions equals the emission decay rates. The inter-system crossings are determined by the rates:

$$(k_{z^0s}, k_{x^0s}, k_{y^0s}), (k_{sz}, k_{sy})$$

There are no reverse terms associated with the inter-system crossing and, hence, the related parameters with the indices reversed are zero. Likewise all the relaxation rates between the spin levels z, x and y and between levels  $z', x'$  and  $y'$  are small. These parameters can be considered equal and given a small value but the effects are not significant in the calculated responses.

Here a sample has been in the dark for a period long compared to the spin-lattice relaxation time the population will initially be equally distributed over the three ground state spin levels, z, x and y. Emission is established in a time of the order of the excited state lifetime of 10–20 ns and with continuing excitation the emission level increases as population is transferred to the z state (Fig.8). This behavior is in correspondence with observation (Fig.4). However, little significance can be drawn as there has not been an independent measurement of the optical pumping rate and the magnitude of the rise in Fig.4 has been used in determining the parameters of the system.

Other than the optical pumping rate there are no free parameters when calculating the emission associated with the dual pulses experiments. In these experiments the intensities are high and the transfer of population into the singlet level is initially faster than the relaxation from the singlet to the ground state. Consequently there is a build up of singlet population and associated with this there is a drop in the emission level. The situation is calculated for a light field switched on and held constant for 1 s, switched off for 1 s and then switched on again for a further 1 s. With the intense excitation the system reaches equilibrium during the 1 s pulse and so is spin polarized well before the end of the first pulse. In the dark period there is a relaxation of the singlet

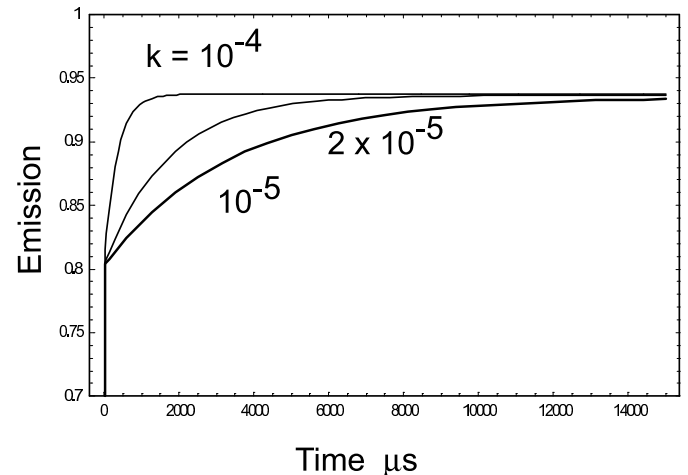


FIG. 8: Emission calculated from solution of the rate equation for energy scheme in Fig 2. The intensities  $k$  are given in units of  $1/\mu\text{s}$ . The value of the parameters in units of  $10^6 \text{ s}^{-1}$  introduced in the text are  $k_{zz^0} = k_{xx^0} = k_{yy^0} = 77$ ;  $k_{sz} = 3.3$ ,  $k_{sx} = k_{sy} = 0$ ;  $k_{z^0s} = 0$ ;  $k_{x^0s} = k_{y^0s} = 30$ ;  $k_{zx^0} = k_{zy^0} = k_{xz^0} = k_{yz^0} = 1.5$

population but there is no loss in spin-polarization. The result is that for the second light pulse the system starts spin polarized with a preferential population in the z spin ground state. In this case the transfer to the singlet is less efficient and the build up of population in the singlet level is slower. This accounts for the observed slower drop in emission intensity with the second pulse. The behavior for representative intensities are shown in Fig. 9.

The results of the calculations can be compared with the experimental measurements of Fig 6. It should be recognized that the calculations are for a simpler situation than realized experimentally. The calculations are for an ensemble of identical centers with identical optical pumping rates whereas the experiment involves four orientations and variation in the optical pumping rates. The consequence of these factors can be approximated by adding a square wave emission response to the calculated emission response before comparing with experiment. The structured component of the response (the "peak") will then represent a smaller fraction of each pulse. Another important consideration is that photo-ionization has not been included. In the calculations the peak of the second pulse is stronger than that of the first whereas it is the reverse in the experiment. The difference is due to photo-ionization. Photo-ionization causes there to be a reduction in the number of N-V centers during the first pulse (giving small alteration to the slope). The recovery is slow and there is no recovery during the short dark period. Hence, the number of centers involved is larger at the start of the first pulse than at the start of the second pulse. When allowing for these factors and recognizing that the parameters have been determined from independent measurements the correspondence between the calculated responses in Fig.9 and equivalent

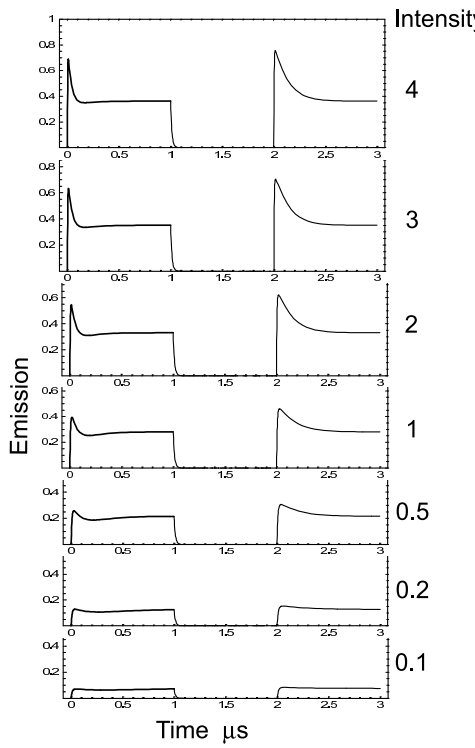


FIG . 9: (a) Em ission predicted from the solution of the rate equations for a pair of excitation pulses. The em ission is shown for various excitation intensities  $k$  shown on the right in units of  $1/\mu\text{s}$ . The value of the parameters are given in the text and summarized in the caption of Fig 8.

experimental traces in Fig.6 are very satisfactory.

## V I. M A G N E T I C F I E L D C A L C U L A T I O N

A magnetic field other than along the trigonal axis causes mixing of the spin states [15] and consequently with a randomly oriented field the populations are not associated with separate  $z$ ,  $x$  and  $y$  states. The effect can be approximated by retaining equal populations in the three spin projections and the result of doing this is shown in Fig 10. The upper trace gives the response in the absence of a magnetic field and is the same as in the previous section with  $k = 1$ . For the lower trace the populations in the three ground spin states are equalized. When this is done to approximate the effect of a magnetic field, there is no spin polarization and the responses are the same for the two pulses. With the field applied there continues to be optical excitation from the  $x$ ,  $y$  state and more efficient transfer into the singlet level. The result is that the equilibrium population in the singlet level is higher and less centers contribute to the emission. The final emission is lower and this is what is observed. It should be noted that equivalent effects can be obtained by applying resonant microwave fields to maintain population in the  $x$ ,  $y$  states. At high intensities the drop in

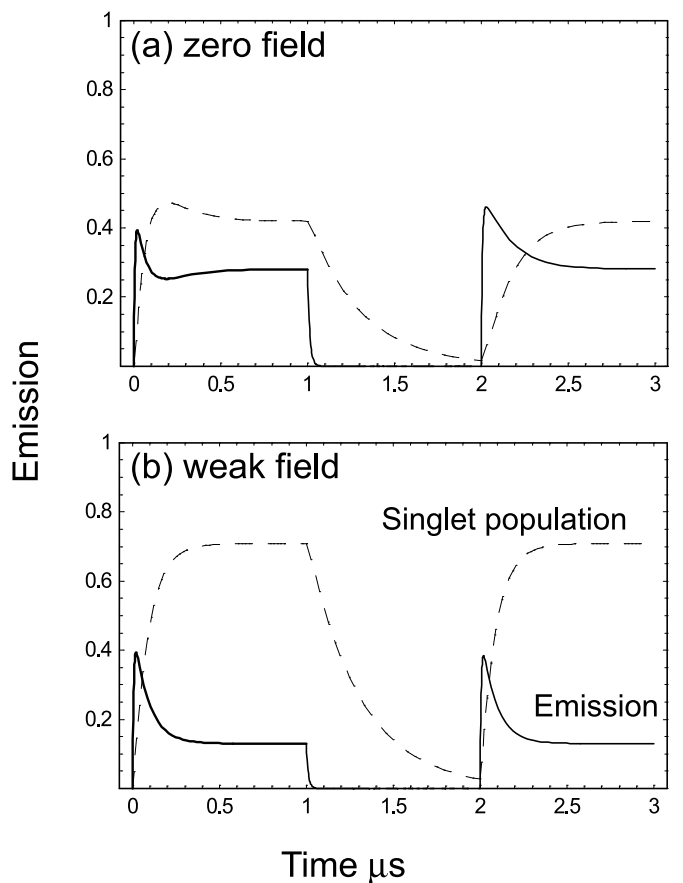


FIG . 10: Em ission predicted from solutions of rate equations illustrating effect of an applied magnetic field. The solid line in the upper trace shows the em ission of system determined from solution of rate equations for energy scheme as shown in Fig 2. The dashed line indicates the variation in population of singlet level. For the lower trace the three ground states are mixed, effectively maintaining equal population in the three spin projections. The excitation rate is  $k = 1$  in units of  $1/\mu\text{s}$ . The value of the parameters are given in the text and summarized in the caption of Fig 8.

equilibrium em ission level caused by the microwave field can be much larger [39] than the 14% obtained at low intensities. This is due to the change of the population stored in the singlet level.

In comparing the responses with and without an applied magnetic field it can be observed that there is a variation in the magnitude of the peaks. The peak in the em ission associated with the first pulse is similar with and without field. However, the magnitudes associated with the second pulse are very different. As discussed previously, the difference in peak heights between first and second pulses is due to photo-ionization varying the number of centers. A smaller second peak indicates that the magnetic field has caused an increase in the photo-ionization. This can be attributed to the field increasing the population in the excited states (excited triplet plus singlet) and the ionization being out of these states. It

is desirable to establish whether the ionization occurs through tunnelling out of these states or is light induced. This requires further investigation.

## VII. COMPARISON WITH OTHER WORK

There have been many publications referring to the singlet level in the N-V center and many of these publications give information that is in conflict with the current model. The disparities are discussed below.

In this work it is shown that the singlet has a short lifetime of 0.3 s. This contrasts to the value of 0.275 s given when an intermediate  $^1A$  singlet was first proposed. Redman et al. [18] suggested that a long lived electronic state could account for a 12 Hz resonance observed in near degenerate 4-wave mixing. However, it was recognized that the narrow resonance could be associated with a long lived spin, rather than electronic, state and a spin-lattice relaxation time of 0.275 s is quite realistic for N-V centers in diamond. Should the resonance be reassigned to the spin state then their data can be explained without invoking a long lived singlet state. This would then be consistent with the present model.

The presence of a long lived singlet has also been adopted to account for the loss of emission from single centers as the temperature is lowered [2, 3]. The emission is from the excited state, but it was considered that there could also be decay to a long lived dark state. Some of the emission would be lost unless there was back transfer from the dark state. Assuming this back transfer is thermal it would be less efficient as temperature is lowered and there would be an associated loss in emission intensity. The experiments involved exciting single centers using wavelengths within the zero-phonon line but, should the above explanation be correct, there would be an equivalent loss with excitation within the vibronic band. This is not the case as there is little change in emission intensity with a lowering of temperature (see Fig 3). The more likely explanation is that the loss is associated with spectral hole-burning. There are a range of processes (change of spin state, re-orientation of center or movement of charge in the neighborhood of the center) which can shift the absorption frequencies of individual centers and cause a decrease of absorption at the

fixed laser frequency. This will result in loss of emission which will become pronounced as the homogeneous line width of the zero-phonon line decreases with decreasing temperature. Accounting for the loss of emission as due to hole-burning means that other conclusions have to be modified. For example, if the loss of emission with temperature is not associated with a singlet level the data cannot be used to give information about the position of any levels [3, 40]. In the present model there is a singlet and there is decay into this singlet. However, back transfer is not an issue. Because of the short lifetime when the excitation is weak there is negligible population in the singlet that can be involved in back transfer. When

the intensity of excitation is high and an average population is retained in the singlet there could be back transfer. However, the behavior of the system has been satisfactorily modelled neglecting back transfer and so it is not a processes essential for understanding the dynamics of the system.

In association with back transfer from the singlet to the  $^3E$  state it is often assumed that there is no decay from the singlet to the ground state [4, 5]. In this case the spin polarization would have to arise through the back transfer and be strongly temperature dependent. This is not what is observed. Spin polarization occurs from liquid helium temperatures to room temperatures and in the original measurements of spin polarization Lousser and van Wyk [15] have shown that the polarization is maintained to 500 K. Another more important issue is accounting for how the spin polarization could arise through a thermal back transfer process. No details have been presented as to how this could be achieved. This is in contrast with the present model where, rather than back transfer, there is decay from the singlet direct to the ground state. With the decay channels proposed one can readily account for the spin polarization. It can be concluded that the N-V center can be understood without back transfer playing a role.

It is noted that the analysis of the photon statistics associated with emission from single N-V centers [2, 3, 4, 5, 30] has assumed that either there is significant singlet-triplet back transfer or a long lived singlet state (or both). Consequently the parameters reported are inconsistent with the values obtained here. Such measurements need to be re-analyzed using the present model and consideration given to possible contributions of photo-ionization effects.

The notation for the electronic states and rate parameters was deliberately chosen to facilitate comparison with those given by Wachter and co-workers at University of Stuttgart and at the National Academy of Sciences of Belarus. They have presented an exciting range of single site measurements demonstrating aspects of quantum computing [7, 8, 9, 10, 11, 30, 31, 42, 43]. In their model of the center they have considered that spin is a good quantum number and spin-orbit interaction is neglected so that all optical transitions conserve the spin projection. However, the justification for the very weak spin-orbit interaction is based on other work [27] where use is made of a high symmetry commutation relationship not valid in the present system. Therefore, it is doubtful that spin-orbit can be neglected and in the present model it is found to play a role in accounting for experimental data. Nevertheless the energy level diagram and the selection rules they have adopted are similar to that obtained here in our case of low symmetry. There are similarities in the values of some of the parameters. For example, we have determined that the rate constant for inter-system crossing from the excited  $x'y'$  states to the singlet  $s$  has a value of  $k_{x^0s} = k_{y^0s} = 0.39 \times 1/$ . This is in good correspondence with a value of  $0.5 \times 1/$  given by Nizovtsev

etal. [31]. They have also proposed that there is much slower transfer from the  $^3E$   $z'$  state to the singlet and we agree with this conclusion. They have given a value of  $k_{z^0s} = 0.02 \times 10^6 \text{ s}^{-1}$ . In our model it is considered to be zero but a small value such as they have given does not change the behavior of the system. There is, therefore, reasonable agreement for the populating of the singlet level. However, there is little correspondence for transfer out of the singlet level and the situation is confused. Part of the difficulty arises from taking the singlet to have the long 0.275 s lifetime and neglecting decay from the singlet direct to the ground state [31]. The transfer out of the singlet giving rise to the spin polarization has then to be through thermal back transfer to the excited triplet plus optically driven processes presumably involving higher excited state levels. This latter process is inconsistent with the observation that the spin polarization is linear [23, 41]. Also to fit experimental data optically driven transfer from the triplet to the singlet has been included. As there are no such processes in our model there can be no comparison with the parameters given.

In other work [9, 29, 30, 43] direct transfer from the singlet to the ground state is indicated and it is considered that the spin polarization can arise in this way. Mention has also been made of the singlet having a short lifetime [43]. There is then good correspondence with the present model although parameters have not been given to enable a detailed comparison. There has been a focus on accounting for a single sharp zero-phonon line in the excitation spectrum of a single N-V center. This is a very significant observation as it is crucial for the use of the N-V center for many quantum information processing applications. Detection requires there to be a transition that cycles without change of spin projection and their observation indicates that the  $z \leftrightarrow z'$  transition can cycle 100,000x. This is in contrast to that indicated by our model where with present parameters the cycling of the  $z \leftrightarrow z'$  transition would be limited to 50x on average. In the model the cycling is limited by the non-spin-conserving optical transitions and, as noted earlier, the strength of these transitions vary significantly with strain. They depend on the separation of  $S_z$  and  $(S_x, S_y)$  spin levels in the excited state and the separation varies from 1 GHz with strain to 30 GHz without strain. Therefore, there can be a factor of 30x variation in the mixing and a  $10^3$  variation in strength of the transitions between centers at strained and non-strained sites. Our ensemble-based measurements favor the strained situation and so our parameters correspond to those for a center in a large strain field. Much larger 50,000x cycling could be expected for centers with minimal strain and as this is reasonably consistent with their observations it is concluded that their experiments are likely to involve sites with low strain. With this interpretation our model is valid though it must be appreciated that the strength of the non-spin-conserving transitions vary significantly from site to site and the value we give is for an ensemble average favoring strained sites.

Loss of cycling implies there is hole burning and hole burning will, therefore, favor strained sites for which the non-spin-conserving optical transitions are stronger. A strain also shifts the position of the zero-phonon line it is expected that hole burning will be associated with sites away from the center of the zero-phonon line. This is in general what has been reported. For the opposite situation to have cycling requires less strained sites and these are likely to have frequencies close to the center of the inhomogeneously broadened zero-phonon line. This is what is reported where single sites have only been observed for a narrow band of frequencies near the line center. The difference in the sites selected by hole-burning and single center experiments have been identified previously [2] and this work provides some insight as to the origin of the variation.

The conditions for the observation of zero-phonon lines are restrictive. Clearly it requires the strain to be small but as yet there is no knowledge as to how a quantitative measure can be made. From the model it can be seen that it requires very little mixing of the spin states to affect the detection. For example, transverse magnetic fields of only a few gauss are sufficient to reduce the reported cycling and degrade the detection efficiency. On the other hand the variation of properties site to site is an exciting aspect as it may enable sites to be obtained with specific properties and this work will allow us to anticipate what properties might be achievable. For example, it is straightforward to see how it is possible to obtain sites with a configuration. The intention would be to identify properties that are well matched to particular applications.

### V III. CONCLUSION

In this work group theoretical considerations have been used to account for the states of the N-V center, for the optical transitions and for the inter-system crossing. The account leads to a seven level model where the dynamics are dominated by four rate constants. These four rate constants are determined from experimental measurements and it is shown that with these values the model gives very good correspondence with experimental measurements of ensembles. The comparison between theory and experiment is not fully quantitative but the agreement is sufficient to give confidence in the appropriateness of the model. A good physical understanding of the response of the center to optical excitation is obtained and the significance is that the model provides a basis for the development of N-V center applications and for strategies to target the significant parameters.

### IX. ACKNOWLEDGMENTS

The above work has been supported by a DARPA QuIST grant through Texas Engineering Experimental

Station and by Australian Defence Science and Technology Organisation. The authors thank Professors Philip

Hemmer (Texas A & M University) and Fedor Jelezko (University of Stuttgart) for useful discussions.

---

[1] A. Gruber, A. D. Rabenstedt, C. Tietz, L. Fleury, J. Wachtrup and C. von Borczyskowski, *Science* 276, 2012-2014 (1997)

[2] A. D. Rabenstedt, C. Tietz, J. Jelezko, J. Wachtrup, S. Klin and A. N. Izovtsev, *Acta Physica Polonica A*, 96, 664-674 (1999)

[3] A. D. Rabenstedt, L. Fleury, C. Tietz, J. Jelezko, S. Klin, A. N. Izovtsev and J. Wachtrup, *Phys. Rev. B*, 60, 11503-11508 (1999)

[4] C. K. Urtsiefer, S. M. Ayer, P. Zarda, H. W. Einfurter, *Phys. Rev. Lett.* 85, 290-293 (2000)

[5] R. Brouri, A. Beveratos, J.-P. Poizat, and Philippe Grangier, *Opt. Lett.* 25, 1294-1296 (2000); A. Beveratos, S. Kuhn, R. Brouri, T. Gacoin, J.-P. Poizat and P. Grangier, *Eur. Phys. J. D* 18 191-196 (2002); A. Beveratos, R. Brouri, T. Gacoin, J.-P. Poizat and P. Grangier, *Phys. Rev. A*, 64, 061802(R) (2002)

[6] A. Beveratos, R. Brouri, T. Gacoin, A. Villing, J.-P. Poizat, P. Grangier, *arXiv:Quant-ph* 2061361v1

[7] J. Wachtrup, S. Ya. Klin and A. P. N. Izovtsev, *Optics and Spectroscopy*, 91, 429-437 (2001)

[8] F. Jelezko, I. Popa, A. Gruber, C. Tietz, J. Wachtrup, A. N. Izovtsev, S. Klin, *Appl. Phys. Lett.* 81 2160-2162 (2002)

[9] F. Jelezko, T. Gaebel, I. Popa, M. Domhan, A. Gruber, J. Wachtrup, *Phys. Rev. Lett.* 93 130501 (2004)

[10] F. Jelezko, J. Wachtrup, *J. Phys.: Condens. Matter* 16 R 1089-1104 (2004)

[11] F. Jelezko, T. Gaebel, I. Popa, A. Gruber, J. Wachtrup, *Phys. Rev. Lett.*, 92 076401 (2004)

[12] L. du Preez, Thesis, University of the Witwatersrand, Johannesburg (1965)

[13] G. Davies and M. F. Hamer, *Proc. R. Soc. Lond. A* 348, 285-298 (1976)

[14] J. W. Steeds, S. Charles, T. J. Davies, A. Gilmore, J. Hales, D. Pickford, J. E. Pickford, *Diamond and Related Materials*, 8, 94-100 (1999)

[15] J. H. H. Loubser and J. A. van Wyk, *Diamond and Research* 1, 11-15 (1977)

[16] N. R. S. Reddy, N. B. M. Anson and C. Wei, *J. of Luminescence* 38, 46-47 (1987)

[17] E. van Oort, N. B. M. Anson and M. G. lasbeek, *J. Phys. C: Solid State Phys.* 21 4385-4391 (1988)

[18] D. A. Redman, S. Brown, R. H. Sands and S. C. Rand, *Phys. Rev. Lett.* 67, 3420-3423 (1991)

[19] N. B. M. Anson, P. T. H. Fisk and X.-F. He, *Appl. Magn. Reson.* 3 999-1019 (1992)

[20] A. Lenef, S. W. Brown, D. A. Redman, S. C. Rand, J. Shigley and E. Fritsch, *Phys. Rev. B*, 53, 13427-13455 (1996); A. Lenef and S. C. Rand, *Phys. Rev.*, 53, 13441-13454 (1996)

[21] J. P. Goss, R. Jones, P. R. Briddon, G. Davies, A. T. Collins, A. Mainwood, J. A. van Wyk, J. M. Baker, M. E. Newton, A. M. Stoneham and S. C. Lawson, *Phys. Rev. B*, 56, 16031-16032 (1997); A. Lenef and S. C. Rand, *Phys. Rev. B*, 56 16033-16034 (1997)

[22] C. A. Coulson and M. J. Kersley, *Proc. R. Soc. London, A*, 241, 433 (1957)

[23] J. P. Harrison, M. J. Sellars and N. B. M. Anson, *J. Luminescence*, 107 245-248 (2004)

[24] R. T. Harley, M. J. Henderson, and R. M. Macfarlane, *J. Phys. C: Solid State Phys.*, 17, L233-L236 (1984)

[25] D. Redman, S. Brown and S. C. Rand, *J. Opt. Soc. Am. B*, 9, 768-774 (1992)

[26] N. B. M. Anson and C. Wei, *J. of Luminescence*, 58, 158-160 (1994)

[27] J. P. D. Martin, *J. of Luminescence* 81 237-247 (1999)

[28] J. P. Goss, R. Jones, S. J. Breuer, P. R. Briddon and S. Oberg, *Phys. Rev. Lett.* 77, 3041-3044 (1996)

[29] A. P. N. Izovtsev, S. Ya. Klin, F. Jelezko, I. Popa, A. Gruber and J. Wachtrup, *Physica B* 340-342, 106-110 (2003)

[30] A. P. N. Izovtsev, S. Ya. Klin, F. Jelezko, I. Popa, A. Gruber, C. Tietz and J. Wachtrup, *Optics and Spectroscopy* 94, 848-858 (2003)

[31] A. P. N. Izovtsev, S. Ya. Klin, F. Jelezko, T. Gaebel, I. Popa, A. Gruber and J. Wachtrup, *Optics and Spectroscopy* 99, 233-244 (2005)

[32] G. Davies, *J. Phys. C: Solid State Phys.*, 7, 3797-3809 (1974)

[33] N. B. M. Anson, J. P. Harrison, Diamond and Related Materials, 14, 1705-1710 (2005)

[34] T. Gaebel, M. Domhan, C. Winnmann, I. Popa, F. Jelezko, J. Rabeau, A. Grangier, S. Pravert, E. Trajkov, P. R. Hemmer and J. Wachtrup, *Appl. Phys. B DOI: 10.1007/s00340-005-2056-2* (2005)

[35] G. Davies, *J. Phys. C: Solid State Phys.*, 12, 2551-2566 (1979)

[36] A. T. Collins, M. F. Thomas and M. I. B. Jorge, *J. Phys. C: Solid State Phys.*, 16 2177-2181 (1983)

[37] H. Hanazana, Y. Nishida, T. Kato, Diamond and Related Materials, 6 1595-1598 (1997)

[38] J. Harrison, M. J. Sellars and N. B. M. Anson, Diamond and Related Materials, (2005) to be published

[39] F. Jelezko, private communication.

[40] F. Jelezko, T. Tietz, A. Gruber, I. Popa, A. N. Izovtsev, S. Klin and J. Wachtrup, *Single Molecule* 2 255-260 (2001)

[41] I. Hirotsu, J. Wachtrup and M. G. lasbeek, *Phys. Rev. B*, 46, 10600-10612 (1992)

[42] I. Popa, T. Gaebel, M. Domhan, C. Winnmann, F. Jelezko and J. Wachtrup, *arXiv:quant-ph/0409067* (2004)

[43] J. Wachtrup and F. Jelezko, *arXiv:quant-ph/0510152* (2005)